JOM, Vol. 72, No. 9, 2020
https://doi.org/10.1007/s11837-020-04257-7

Confirmation of Anomalous Nucleation in Zirconium

G.P. BRACKER,[1,4] S. SCHNEIDER,[2] R. WUNDERLICH,[3] H. FECHT,[3] J. ZHAO,[1] and R.W. HYERS[1]

1.—University of Massachusetts Amherst, Amherst, USA. 2.—Deutsches Zentrum für Luft- und Raumfahrt, Cologne, Germany. 3.—Ulm Universität, Ulm, Germany. 4.—e-mail: gbracker@umass.edu

Pure, low-oxygen zirconium samples have been observed to nucleate a solid phase under conditions during which the sample was expected to remain liquid. This phenomenon was first seen during Spacelab Mission MSL-1R (materials science laboratory) experiments and has since also been observed in the International Space Station (ISS) electromagnetic levitation (EML) facility on a different sample. Current work has been able to replicate these anomalous solidification events under a range of conditions in the ISS MSL-EML facility. The solidification events are not well explained by classical homogeneous or heterogeneous nucleation. The current theory is that collapsing voids in the melt create a local region of high pressure that results in local material being deeply undercooled and a strong driving force for solidification.

INTRODUCTION

The transformation between the noncrystalline melt structure and the crystalline solid has been well studied in liquid metals. The solidification begins at a nucleation site from which a crystalline solid grows. These nucleation sites can originate either homogeneously in the melt or heterogeneously on a site that reduces the critical volume of the nucleus to initiate growth. The rate of formation of these nucleation sites depends on the free energy of the system, temperature, atomic vibration frequency, activation energy, and other factors. In non-glass-forming liquid metals, the rate of nucleation is heavily dependent on temperature, increasing rapidly from functionally zero to nearly instantaneous over a very narrow temperature range.[1]

The specifics of free energy and temperature at which this increase occurs depends on the properties of the melt and solid crystal. During solidification, heterogeneous nucleation typically dominates the formation of nuclei because the heterogeneous nucleation sites reduce the free energy required to form a nuclei with a supercritical radius to allow for growth.[1]

However, heterogeneous nucleation can be minimized using levitation techniques in a vacuum. Electromagnetic levitation (EML) is one such technique that utilizes a magnetic field to control the position of the sample and to induce heating in the sample. During electromagnetic levitation in vacuum, the magnetic levitation eliminates contact with the container and a gas, minimizing heterogeneous nucleation sites. This allows access to deep undercoolings, often on the order of 200°C–300°C or more.[2] During electromagnetic levitation (EML) processing, it is typically expected that a subcritically undercooled melt can be held at constant, subcritical, undercooling for hours without solidification occurring.[3–5]

High-purity zirconium was shown to achieve 334° ± 4°C undercooling in 110 free-cooling EML cycles in vacuum in reduced gravity by Hofmeister et al.[2] However, in six cycles the sample was held at smaller undercoolings and solidified on the order of 10 s to 100 s of seconds. The low stability of the undercooled liquid phase is not compatible with the deep undercoolings observed during free cooling and thus considered anomalous. The reported anomalous nucleation was not consistent with chemical contamination as subsequent free cooling cycles again achieved deep undercoolings. Instead, the anomalous solidification events were attributed to dynamic nucleation induced by the collapse of cavities in the fluid[2] similar to the theory presented in Refs. 6 and 7.

(Published online July 6, 2020)

In an undercooled liquid, cavitation can induce nucleation when the cavity collapses. The collapse is followed by a pressure spike accompanied by a shift in the melting point. As described by the Clausius–Clapeyron equation:

$$\ln\left(\frac{P_1}{P_2}\right) = \frac{\Delta H_{\text{vap}}}{P}\left(\frac{1}{T_2} - \frac{1}{T_1}\right)$$

in which P_1 and P_2 are the pressures at temperatures T_1 and T_2, respectively, and ΔH_{vap} is the enthalpy of vaporization. The shift in the melting point results in a much deeper undercooling and, as a result, sufficient driving force for nucleation to occur.[8]

Similar anomalous nucleation was observed 19 years later in a high-purity zirconium sample in a different experimental facility, the MSL-EML (Materials Science Laboratory electromagnetic levitator) onboard the International Space Station (ISS) during additional experiments in June 2016 and July 2018.

The zirconium flight sample used onboard the ISS for MSL-EML processing was cast from bulk metallic glass-quality zirconium in an arc melter into a water-cooled copper mold. The oxygen content of the sample was validated by LECO hot gas extraction analysis, which found the material to contain 0.005 wt% oxygen. During processing in the MSL-EML facility, changes in the width of the solid state $\alpha \rightarrow \beta$ phase transition at $T = 1137$ K indicate that the oxygen concentration had increased to at least 400 wt ppm.[9]

EXPERIMENTAL OBSERVATIONS

The experiments onboard the ISS MSL-EML were done on the same zirconium sample from 2016 to further explore the observed solidification phenomena by exploring the repeatability and work toward quantifying the conditions under which the anomalous nucleation occurs.

In this series of 22 experiments, the sample was melted in vacuum. Of the 22 experiments, 18 cycles held the sample at sub-critical undercoolings, between 45° and 290° undercooled, until nucleation occurred at isothermal holding in < 10 min. The isothermal holds for the cycles of interest are given in Table I in which the cycle number, sequence in the temperature series, and description are given with the undercooling and time to solidification. The undercoolings were chosen to replicate results from experiments done on the same sample in 2016. Additional cycles were done at different undercoolings to sample a broader range of undercoolings. While each target temperature was tested multiple times, the sequence of processing target temperatures in the cycles was deliberately randomized to reveal any effects of processing sequence. These effects are plotted for each separate temperature series in Fig. 1 and against the overall series of experiments in Fig. 2. It should be noted that in Figs. 1 and 2, only the cycles that solidified during the isothermal hold have been plotted for consideration and the free cooling cycle is not included in the analysis of sequencing effects.

The data were evaluated to determine if there was a trend relating the time to solidification and the sequence in which cycles were run. By plotting the time to solidification against the sequencing number for each temperature set, Fig. 1 allows the effects of run order to be observed for each individual temperature series and fails to find a consistent pattern of sequencing effects. Additionally, Fig. 2 plots the overall series of experiments against the time to solidification. To quantify the effects of sequencing on the time to solidification, the correlation coefficient was calculated for the cycle number and time to nucleation. The correlation coefficient was found to be 0.385, which fails to support a correlation between the time to solidification and cycle number. Furthermore, this lack of correlation indicates that there are no discernable changes in heterogeneous nuclei in the sample during the experiments of interest.

During the experiment, the sample was levitated to maintain isothermal holds in which the flow was driven by both the positioner and the heater circuits. The applied heater current results in much higher flow velocities, given in Figs. 3 and 4, than allowing the sample to free cool. During the isothermal holds, the maximum velocity in the drop is between 0.137 m/s and 0.209 m/s. In these cycles the time to solidification is variable within the range of 1 s to 576 s. Figure 1 shows that the variation in time to solidification does not correspond to the undercooling. The different undercoolings are isothermal holds; therefore, the flow conditions are identical for a given targeted undercooling. Therefore, the same conclusion applies to flow: the stochastic variation under identical conditions is larger than the variation due to stirring in the experimental range.

The internal flow of the drop has been quantified and characterized using computational fluid dynamics (CFD), which allows the properties of the flow to be calculated from the thermophysical properties of the melt[10,11] and applied EML force field. The models have been validated against a prior sample of CoCu in which the flow was directly observable through the difference in emissivity of the two-phase liquid present in the sample during melting.[12] The flows in all the experiments are characterized by Reynolds numbers > 600, which is considered the limit of laminar flow in EML; above this the flow is characterized as turbulent.[13]

The flow was calculated for the cycles with the smallest and largest undercooling, i.e., $\Delta T = 47$ K and $\Delta T = 293$ K, respectively, to characterize the Reynolds numbers and local pressure within the drops during the isothermal holds. During the cycles with the largest undercooling, the maximum velocity within the sample was 0.137 m/s, shown in

Table I. Experimental cycle overview for processing zirconium onboard ISS MSL-EML during Batch 1.3 in August 2018

Cycle number	Sequencing number	Hold	Undercooling	Time to solidification
61	1	Isothermal hold	191.1	8 s
62	2	Isothermal hold	178.3	1 s
63	3	Isothermal hold	187.7	43 s
64	4	Isothermal hold	192.8	152 s
65	5	Isothermal hold	188.6	49 s
66	6	Isothermal hold	193.3	241 s
67	7	Held for 227 s at $\Delta T \sim 180$, then free cool**	313.1	–
70	1	Isothermal hold	65.7	15 s
71	1	Isothermal hold	115.8	36 s
72	1	Isothermal hold	246.5	508
73	1	Isothermal hold	293	576 s
74	1	Isothermal hold	47.1	137 s
75	2	Isothermal hold	70.8	189 s
76	2	Isothermal hold	117.0	305 s
77	–	Free cooling	324.3	–
78	3	Held for 223 s at $\Delta T \sim 105$, then free cool**	325	–
79	3	Isothermal hold	72.0	281 s
80	2	Held for 600 s at $\Delta T \sim 235$, then free cool*	324.3	–
81	2	Isothermal hold	286.6	30
82	2	Isothermal hold	50.3	212
83	4	Isothermal hold	67.4	387 s
84	4	Isothermal hold	122.9	180 s

*Cycle timed out and the sample was allowed to free cool.**Cycles were stopped for the safety of the facility.

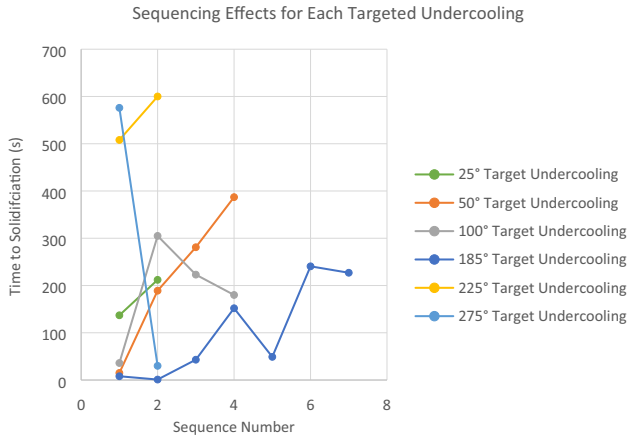

Fig. 1. Sequencing versus solidification time for cycles at different targeted undercoolings. There is no consistent pattern of time to solidification based on the run order for the targeted undercooling temperatures.

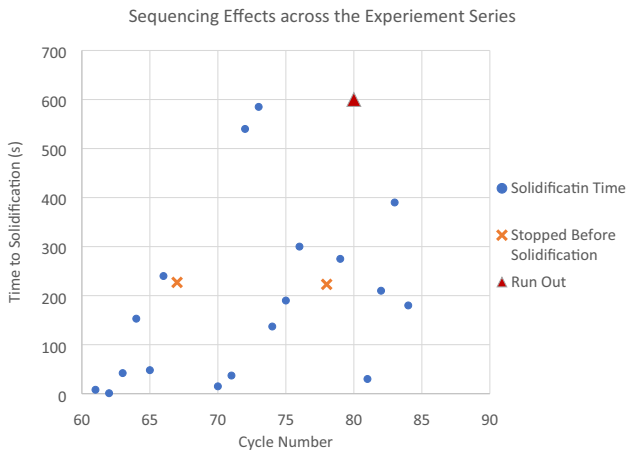

Fig. 2. Changes in the sample can be detected by determining if there is a correlation to any changes in the sample behavior with the sequence order of the experiments. For these experiments, the correlation coefficient was calculated to be 0.385, which fails to provide strong evidence for changes in the sample.

Fig. 3, which resulted in a Reynolds number of approximately 987, which is well above the laminar-turbulent transition. During the cycles with the smallest undercooling, the maximum velocity within the sample was 0.209 m/s, shown in Fig. 4, which resulted in a Reynolds number of approximately 1906, which is well above the laminar-turbulent transition. Across all cycles, the flow inside the drop has been characterized as turbulent.

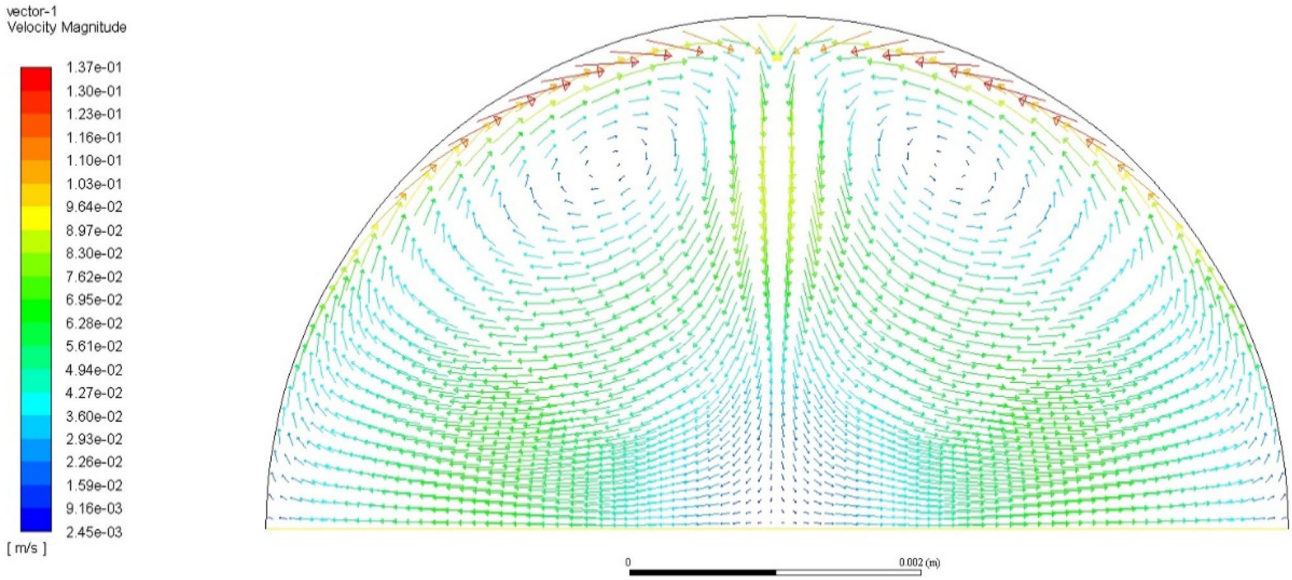

Fig. 3. Velocity vector field calculated using the RNG k-ε turbulence model for Zr at ΔT = 293 K undercooling in an EML field consisting of a 3.43 V heater and 7.03 positioner.

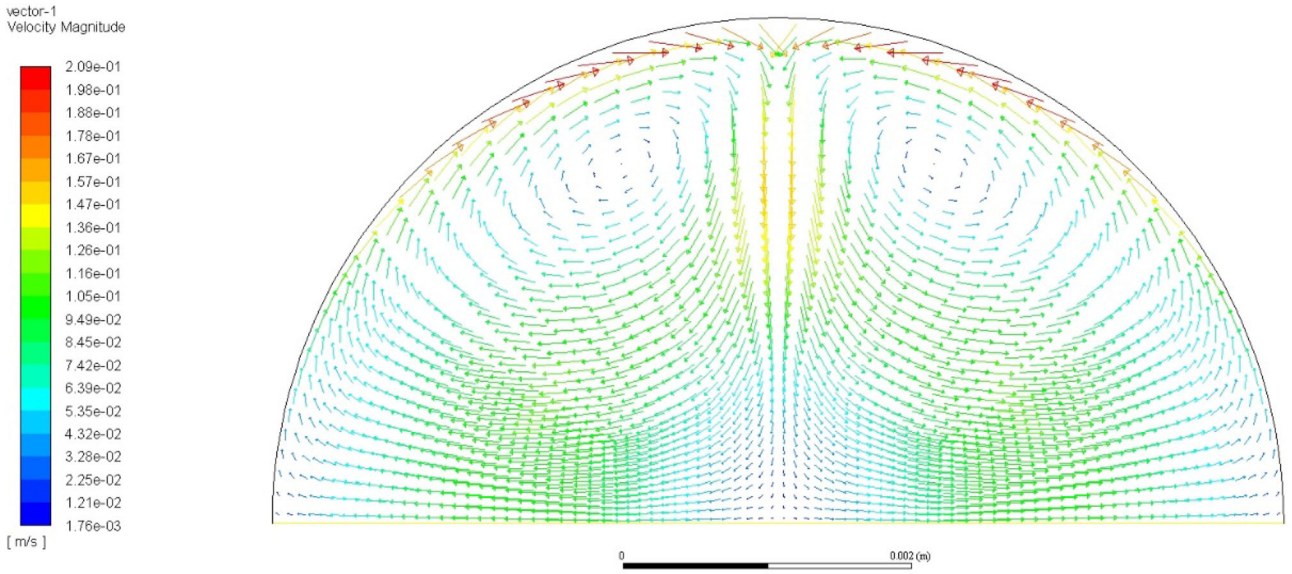

Fig. 4. Velocity vector field calculated using the RNG k-ε turbulence model for Zr at ΔT = 47 K undercooling in an EML field consisting of a 4.92 V heater and 7.03 positioner.

During four cycles, the sample was free cooled and achieved much deeper undercoolings than were observed during cycles with an isothermal hold. In these cycles, undercoolings between 313° and 325° were observed, indicating that the sample remained quite pure or that any dissolved oxygen has little influence on the nucleation behavior. The EML field was dominated by the positioner field and did not have a strong heating field applied to the sample. As a result, the flow was much slower than observed in other cycles. The flow was modeled over the range of cooling to establish the minimum flow in the drop over the experiments at all temperatures and is plotted in Fig. 5, where it can be seen that the laminar model gives Reynolds numbers much larger than the expected laminar-turbulent transition. As a result, the RNG k-ε turbulence model is used to characterize the properties of the flow within the drop. The flow at recalescence is plotted in Fig. 6 where it can be seen that the maximum velocity in the drop is 0.071 m/s using the RNG k-ε turbulence model. In this "low" flow regime, anomalous nucleation events were not observed in these experiments or in similar free-cooling cycles in other experiments.

DISCUSSION

Several different mechanisms have been proposed to explain the solidification phenomena that have been observed in this pure zirconium sample. These mechanisms include classical nucleation, chemical contamination of the sample, dissolved oxygen, and dust particles providing for external heterogeneous nucleation. However, none of these mechanisms are consistent with the observations of the present experiment.

It is possible to estimate the expected nucleation rate, and from that the time a sample can be expected to be held at a given undercooling. For this system, Klein et al.[14] applied classical nucleation theory to fit the distributions of measured undercooling to determine the unknown constant in the nucleation equation, which accounts for heterogeneous nucleation. For the samples closest to the pure zirconium sample used in the ISS MSL-EML facility, labeled EML in their paper, they determined that the population of undercoolings best fit ΔG^* of 42 kT at an undercooling of 330 K.[14] Taking the corresponding value of $f(\theta)$ gives a result that at 250 K undercooling, the nucleation rate should be lower by a factor of 3×10^{17}. This difference in nucleation rate would result in a corresponding change in time to nucleation, for example, from 1 ms to 1 million years. For cleaner samples, this effect is larger. This calculation confirms the experimental results cited previously: for temperatures above some maximum undercooling, the nucleation rate falls off very rapidly. Nucleation at 250 K on a laboratory timescale cannot occur by the mechanism reported in Ref. 14

One proposed explanation for the anomalous nucleation is that the sample might have been contaminated and the behavior being displayed is a result of classic heterogeneous nucleation. However, the sample was observed to deeply undercool during free cooling cycles before, during, and after the series of experiments investigating this anomalous nucleation event. Any chemical contamination does not explain the anomalous nucleation events observed. Furthermore, pure zirconium in the stable liquid phase is extremely reactive and would likely dissolve any contaminants into solution. Also, if such mechanisms were limiting, deeper undercoolings would not have been observed in subsequent cycles.

Another proposed explanation is that given the high temperature and reactivity of liquid zirconium, dissolved oxygen in the sample may have provided for heterogeneous nucleation sites for with oxygen as the chemical containment. However, this is a special case of the previous point. Zirconium does not form a solid oxide phase until very high oxygen concentration; instead, the oxygen remains in

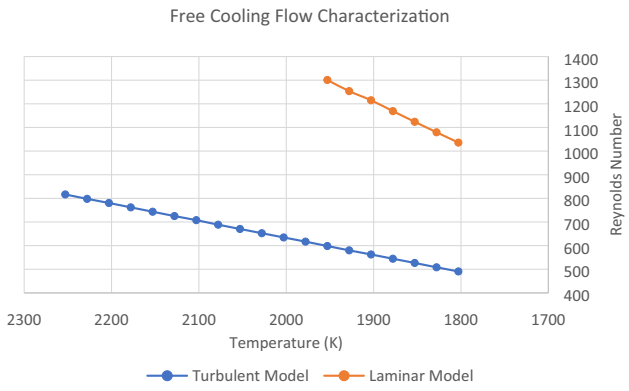

Fig. 5. Flow characterization for free cooling cycles of Zr.

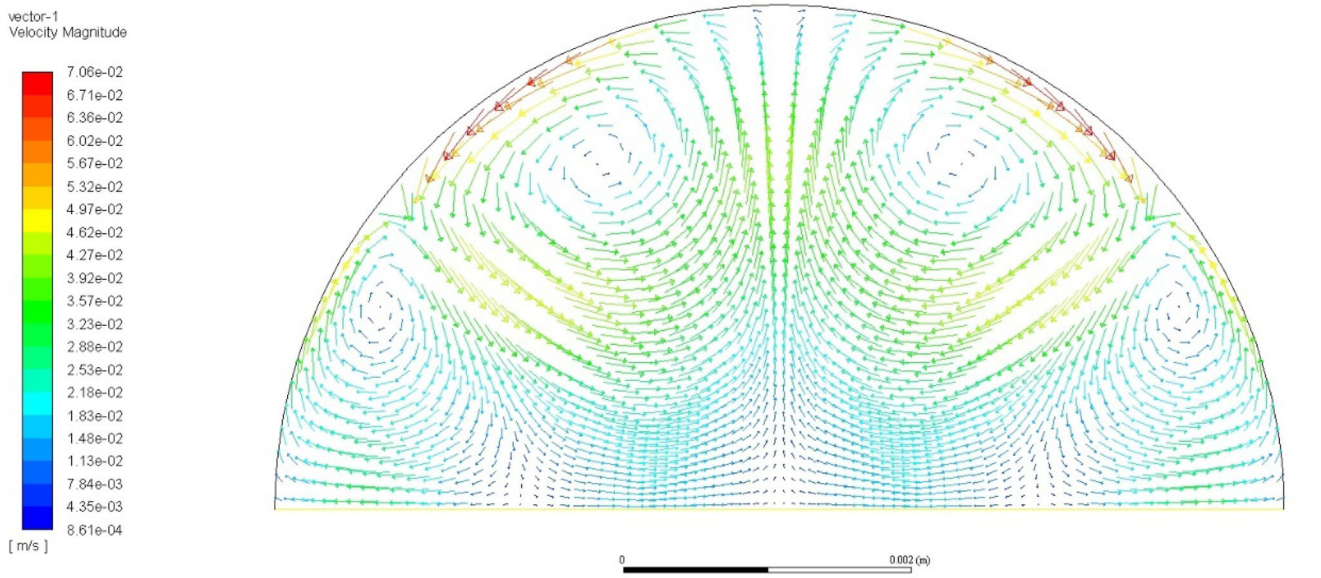

Fig. 6. Velocity vectors calculated for zirconium at 1803 *K* using the RNG k-ε turbulence model.

solution in the metallic phase. While oxygen is known to stabilize the crystalline phase, the inclusion of additional oxygen would result in a few degrees increase in the melting point of the sample. However, the undercooling is measured with respect to the apparent melting point of each cycle. If oxygen contamination resulted in a shift in the melting point, the undercooling would be measured against this shift, which would result in the same undercooling value. Nonetheless, if such an oxide phase were to form during the free cooling cycles, the deep undercoolings would not be achieved. Instead, deep, consistent undercoolings were observed during free cooling.

It has also been suggested that solid "dust" particles in the sample chamber might collide with the sample and provide a heterogeneous nucleation site for solidification to occur. When "dust" forms in EML by condensation of evaporated sample material in the gas phase, the cloud of solid particles is dense enough to be visible to the camera. During the cycles of interest, there was no evidence of such solid particles. Furthermore, the cycles of interest were processed in vacuum, in which the gas necessary for this mechanism is not present. Instead the evaporated material moves radially, away from the sample, until it condenses on a solid surface such as the wall of the chamber, EML coils, sample holder, etc. Larger "flakes" of material in the sample could, in theory, also trigger a heterogeneous nucleation in the sample. However, larger "flakes" are rare in EML and therefore unlikely to account for such a large number of solidification events, even if such "flakes" were present. Also, large flakes were not observed in the video.

The remaining hypothesis is that a form of dynamic nucleation occurs as suggested in Ref. 2 because of mechanisms within the fluid flow of the sample. This hypothesis suggests that a collapsing void within the melt produces a high-pressure shock wave. As a result of the local high pressure generated by the shock wave, the local melting temperature raises, and the local melt experiences a much deeper undercooling. At this deeper undercooling, the driving force for nucleation is substantially larger.

Current work is exploring how the fluid flow and effects of the fluid flow may affect nucleation. Magnetohydrodynamic modeling has been used to calculate and characterize the flow behavior under a range of different conditions. The models show that during the isothermal holds in this zirconium sample, the flow is characterized as turbulent with recirculating loops in the regions of lower EML force fields, shown in Figs. 3 and 4. The reduced hydrostatic pressure due to both the recirculation loops in the main flow and to the rotation of the turbulent eddies could serve to excite oscillations in any void in the liquid that enters these regions of lower pressure.

Voids in liquids are very common, collectively accounting for the excess free volume in the liquid, about 1.6% for molten zirconium.[15] The distribution of these voids has been studied in cooperative liquids[16] and range from the molecular to macroscopic scale. When a void in the melt encounters regions of low pressure, as occurs in the center of turbulent eddies, the void will expand and then collapse as described in Refs. 6, 7 and 17. If the collapse is symmetric, the resulting impact will result in a shock wave. This effect of the shock wave is to cause a small region of very high pressure according to the Rayleigh–Plesset equation, which governs a bubble in an incompressible fluid. This higher pressure, due to the shock wave of the collapse, would elevate the local melting temperature, as is described by the Clausius–Clapeyron equation and consequently results in a much deeper local undercooling and, as a result, a sufficient driving force for nucleation occurs.[8]

Additionally, the CFD allows for the calculation of the internal pressure within the drop. The required pressure for voids to homogeneously nucleate in the melt has been calculated in prior work to be on the order of − 4.5 GPa.[16] In the cycles that solidified on an isothermal hold, the minimum total pressure in the drop was calculated to be between − 90 Pa and − 139 Pa, which is insufficient to cause homogeneous nucleation of critical voids in the melt. At the center of turbulent eddies, the pressure is further reduced by a similar value. Therefore, homogeneous nucleation of voids by this flow is not possible. However, the excitation of existing voids by the transient low pressure due to the flow remains possible. Work on further quantification of this possible explanation for the observed behavior is ongoing.

CONCLUSION

Recent work in 2016 and 2018 has been able to replicate anomalous nucleation events that first occurred during Spacelab Mission MSL-1R in which pure zirconium samples solidified while being held at sub-critical undercoolings. The solidification event occurred both before and after cycles that achieved deep undercoolings, supporting the assertion that the sample has not been contaminated. Additionally, sites for heterogeneous nucleation were not observed in the video evidence of these experiments. As a result, the observed solidification events are not well explained by classical homogeneous nucleation nor heterogeneous nucleation. The current theory is that collapsing voids in the melt create a shock wave and a localized pressure disturbance driving nucleation of the solid.

ACKNOWLEDGEMENTS

The authors thank Jürgen Brillo, Douglas Matson, Dieter Herlach, Ken Kelton, Dirk Holland-Moritz, and Thomas Volkmann for fruitful discus-

sions. The experiment was run in the ISS-EML facility, formerly MSL-EML. Support for this project was provide through NASA Grant NNX16AB40G.

REFERENCES

1. D.A. Porter, K.E. Kasterling, and M.Y. Sherif, *Phase Transformations in Metals and Alloys*, 3rd ed. (Boca Raton: CRC Press, 2009), p. 7–9, 181–246.
2. W.H. Hofmeister, R.J. Bayuzick, R. Hyers, and G. Trapaga, *Appl. Phys. Lett.* (1999). https://doi.org/10.1063/1.123945.
3. D. Holland-Moritz, T. Schenk, P. Convert, T. Hansen, and D.M. Herlach, *Meas. Sci. Technol.* (2005). https://doi.org/10.1088/0957-0233/16/2/007.
4. D.M. Herlach, D. Holland-Moritz, R. Willnecker, D. Herlach, and K. Maier, *Philos. Trans. R. Soc. Lond. Ser. Math. Phys. Eng. Sci.* (2003). https://doi.org/10.1098/rsta.2002.1140.
5. C. Bührer, U. Holzwarth, K.G. Maier, D. Plazek, and J. Reske, *Appl. Phys. A* (1996). https://doi.org/10.1007/BF01567649.
6. J.D. Hunt and K.A. Jackson, *J. Appl. Phys.* (1966). https://doi.org/10.1063/1.1707821.
7. J.J. Frawley and W.J. Childs, *Trans. Metall. Soc. AIME.* 242, 256–263 (1968).
8. J.D. Hunt and K.A. Jackson, *Nature* (1966). https://doi.org/10.1038/2111080b0.
9. R. Wunderlich, Presented at IWG 14, DLR, Colonge, 2016.
10. T. Iida and R.I.L. Guthrie, *The Physical Properties of Liquid Metals* (New York: Oxford University Press, 1988), p. 72.
11. T. Ishikawa, P.-F. Paradis, T. Itami, and S. Yoda, *Meas. Sci. Technol.* (2005). https://doi.org/10.1088/0957-0233/16/2/016.
12. J. Lee, D.M. Matson, S. Binder, M. Kolbe, D. Herlach, and R.W. Hyers, *Metall. Mater. Trans. B* (2014). https://doi.org/10.1007/s11663-013-9995-5.
13. R.W. Hyers, G. Trapaga, and B. Abedian, *Metall. Mater. Trans. B* (2003). https://doi.org/10.1007/s11663-003-0052-7.
14. S. Klein, D. Holland-Moritz, and D.M. Herlach, *Phys. Rev. B* (2009). https://doi.org/10.1103/PhysRevB.80.212202.
15. P.-F. Paradis, W.-K. Rhim, in *Proc. SPIE 3792, Materials Research in Low Gravity II*, 1999. https://doi.org/10.1117/12.351289.
16. J. Zhao, *The Effect of Oxygen on Properties of Zirconium Metal*, Scholarworks @UmassAmherst, 2020. https://scholarworks.umass.edu/dissertations_2/1875. Accessed 9 April 2020.
17. R.W. Hyers, J. Zhao, G.P. Bracker, R. Wunderlich, and H. Fecht, *Light Metals* 100, 1 (2019). https://doi.org/10.1007/978-3-030-05864-7_198.